

 Open access • Journal Article • DOI:10.1002/FLD.916

Shock wave numerical structure and the carbuncle phenomenon — Source link

Yann Chauvat, Jean-Marc Moschetta, Jérémie Gressier

Institutions: École nationale supérieure de l'aéronautique et de l'espace

Published on: 20 Mar 2005 - International Journal for Numerical Methods in Fluids (Wiley)

Topics: Carbuncle

Related papers:

- [A Contribution to the Great Riemann Solver Debate](#)
- [Numerical Instabilities in Upwind Methods: Analysis and Cures for the “Carbuncle” Phenomenon](#)
- [A matrix stability analysis of the carbuncle phenomenon](#)
- [Restoration of the contact surface in the HLL-Riemann solver](#)
- [Approximate Riemann Solvers, Parameter Vectors, and Difference Schemes](#)

Share this paper:    

View more about this paper here: <https://typeset.io/papers/shock-wave-numerical-structure-and-the-carbuncle-phenomenon-5cbkxbsjed>

Shock wave numerical structure and the carbuncle phenomenon

Y. Chauvat, J.-M. Moschetta and J. Gressier*

*Department Models for Aerodynamics and Energetics – ONERA
École Nationale Supérieure de l’Aéronautique et de l’Espace
31400 Toulouse, France*

SUMMARY

Since the development of shock-capturing methods, the carbuncle phenomenon has been reported to be a spurious solution produced by almost all currently available contact-preserving methods. The present analysis indicates that the onset of carbuncle phenomenon is actually strongly related to the shock wave numerical structure. A matrix-based stability analysis as well as Euler finite volume computations are compared to illustrate the importance of the internal shock structure to trigger the carbuncle phenomenon.

KEY WORDS: carbuncle phenomenon, shock-capturing schemes, supersonic flows, Riemann solvers

1. INTRODUCTION

Shock-capturing upwind methods developed since the 1980’s can be classified into two distinct categories: 1. upwind methods which exactly preserve contact discontinuities (which might be referred to as *contact-preserving* methods), 2. upwind methods which introduce spurious diffusivity in the resolution of contact discontinuities. Schemes belonging to the second category never produce the carbuncle phenomenon but are hardly suitable for Navier-Stokes computations (e.g. Van Leer’s method, see Fig. 3(a)) since they artificially broaden boundary layer profiles. On the other hand, schemes taken from the first category are attractive for viscous computations but turn out to be sensitive to the carbuncle phenomenon at various degrees [1] [2] with very few exceptions [3]. It has been recently observed [4] that the internal shock structure is essential to trigger the carbuncle phenomenon. This is consistent with former heuristic explanations for the onset of the carbuncle phenomenon [5] in which intermediate shock points play an important role to generate shock instabilities. In the same way, Karni and Čanić [6] conclude on the influence of the numerical viscosity inside the shock structure. The purpose of the present paper is to investigate the exact influence of the internal shock structure on the carbuncle phenomenon.

*Correspondence to: yann.chauvat@oncert.fr, jean-marc.moschetta@supaero.fr, jeremie.gressier@supaero.fr

2. METHOD

A matrix-based stability analysis [4] has been used to study the occurrence of unstable modes during the shock wave computation. The matrix stability analysis consists of examining the temporal evolution of spatial perturbations of a steady solution prescribed as the initial flow condition. In compact form, the temporal evolution of initial perturbations $\delta\vec{W}_m$ satisfies

$$\frac{d}{dt}(\delta\vec{W}_m) = S \cdot \delta\vec{W}_m \quad (1)$$

A shock instability will be detected if the stability matrix S has at least one eigenvalue whose real part is positive. Matrix S contains all numerical flux gradients at every cell interfaces and also includes the effect of grid distortion and boundary conditions. It should be noticed that the present analysis is continuous in time. Consequently, it does not depend on the time discretization. If an instability is detected, it would occur for any CFL number, even arbitrary small. Results obtained from the matrix-based stability analysis are compared with two-dimensional Euler computations, using a standard finite volume method on structured grids (Figs 3). All numerical methods are first order in time and space since high order reconstruction techniques do not affect the onset of carbuncle solutions.

3. RESULTS

3.1. The normal steady shock wave problem

As a first test case, the analysis is conducted on the simple steady normal shock wave problem. First, a steady one-dimensional solution is obtained with a given upwind scheme. Then, the one-dimensional solution is projected onto a two-dimensional Cartesian grid whose vertical gridlines are aligned with the shock wave. The first step consists of analyzing the capability of numerical fluxes to capture a one-dimensional steady shock wave. For standard shock-capturing finite volume methods, the computation of shock waves may require up to three internal points. Within the contact-preserving schemes family, some schemes, such as Godunov, Roe and HLLC, have at most one intermediate point while Osher's method usually resolve steady shock waves with 2 internal points. In the special case of AUSM-M, a unique internal point value is possible for a given upstream mach number above a limit value: $M_\infty \geq 1.367$. Finally, dissipative schemes usually produce 2 (e.g. Van Leer's method) to 3 internal points (such as Pullin's EFM scheme). In the finite volume method, the cell that contains the shockwave has a state \vec{W}_m which can be interpreted as an average between upstream (\vec{W}_0) and downstream (\vec{W}_1) conservative state vectors

$$\vec{W}_m = \vec{W}_0 + \delta x \left(\vec{W}_1 - \vec{W}_0 \right) \quad (2)$$

where δx is the shock position within the internal grid cell. It is observed that a simple finite volume average of conservative states using the shock position (Eq. 2) is not preserved by any standard schemes. This means that an initially sharp shock wave located at some intermediate position between the upstream cell and the downstream cell will not remain steady but will move toward another intermediate state. This observation appears consistent with the conclusion of Arora and Roe [7] concerning the slowly moving shock problem. Indeed,

during the integration in time, the steady shock wave is the result of a moving shock slowly converging to its final position. Further investigation is certainly needed to establish a closer relationship between both problems. For Roe's method, it has been reported that the internal steady shock point belong to a Hugoniot curve [8] (Fig. 1(a)) defined as

$$\vec{F}_{H1} - \vec{F}_1 = u_{S1} (\vec{W}_{H1} - \vec{W}_1) \quad (3)$$

It turns out that all states obtained from the Hugoniot curve based on the downstream state are left unchanged by contact-preserving schemes which allow one-internal point in the computation of shock waves, i.e. Godunov, Roe and HLLC schemes. The steady intermediate states taken from the Hugoniot curve can be represented as an average between upstream and downstream primitive states:

$$\begin{aligned} \rho_{H1} &= \rho_0 + \alpha_\rho (\rho_1 - \rho_0) \\ u_{H1} &= u_0 + \alpha_u (u_1 - u_0) \\ p_{H1} &= p_0 + \alpha_p (p_1 - p_0) \end{aligned} \quad (4)$$

where

$$\begin{aligned} \alpha_\rho &= \delta x \\ \alpha_u &= 1 - (1 - \delta x) \left(1 + \delta x \frac{M_0^2 - 1}{1 + \frac{\gamma-1}{2} M_0^2} \right)^{-\frac{1}{2}} \left(1 - \delta x \frac{M_0^2 - 1}{\frac{2\gamma}{\gamma-1} M_0^2 - 1} \right)^{-\frac{1}{2}} \\ \alpha_p &= \delta x \left(1 + (1 - \delta x) \frac{\gamma+1}{\gamma-1} \frac{M_0^2 - 1}{M_0^2} \right)^{-\frac{1}{2}} \end{aligned} \quad (5)$$

Any internal shock state can be represented by a set of three components $(\alpha_\rho, \alpha_u, \alpha_p)$ which correspond to a point in the frame illustrated on figure 1(a). During the integration process, any initial intermediate state will converge toward a steady internal shock state which is located along the Hugoniot curve. Thousands of intermediate states randomly chosen inside or outside the cube represented in figure1(a) have been used as initial condition to compute a steady shock solution. After convergence, all points have converged toward the Hugoniot curve. For Van-Leer's method internal converged points belong to a different curve, the upstream internal point lay on the supersonic part and the downstream internal point on the subsonic part of the curve (Fig. 1(b)). Internal points being fully determined (through a single free parameter), one can apply the matrix stability analysis to evaluate the effect of the internal shock wave structure on the carbuncle phenomenon. This is done on a 25×25 Cartesian grid after projecting the steady 1D solution along the horizontal gridlines. For a given upstream Mach number, it can be observed (Fig. 2(a)) that there is a *common critical point* for Godunov, Roe and HLLC schemes, above which the 2D shock remains stable. Furthermore, a stability diagram (Fig. 2(b)) illustrates that : 1. All 2D steady shock waves are stable when the upstream Mach number is less than a value close to 2.0, 2. *even for arbitrary high upstream Mach number*, Godunov, Roe or HLLC methods can produce carbuncle-free solutions, provided that the internal shock point is sufficiently close to the downstream state (Fig. 2(b)).

3.2. The blunt body problem

As a second test case, the supersonic blunt body problem is considered in order to illustrate the importance of the numerical shock structure on the carbuncle phenomenon. The geometry

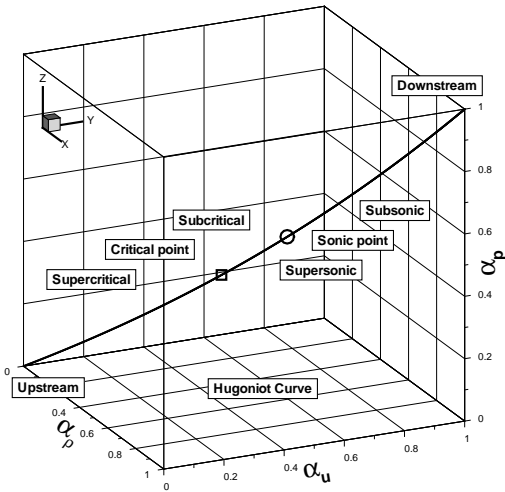
is a half cylinder placed in a supersonic freestream flow at Mach 10. The mesh has 80 cells in the radial direction and 160 along the wall. Van Leer's method is first used to obtain a steady solution with the bow shock located at a certain stand-off distance from the stagnation point. Then, Roe's method is applied using Van Leer's solution as an initial condition to observe the evolution of the shock structure. All computed solutions are double-precision steady solutions in which time residuals have been decreased by 10 orders of magnitude. As expected, Van Leer's method produces a carbuncle-free solution (Fig. 3(a)) while Roe's method produces the carbuncle phenomenon using the same mesh (Fig. 3(b)). When Roe's method is used from Van Leer's converged carbuncle-free solution, the shock wave structure is resolved from two internal points to only one. The interesting observation is that depending on the initial shock wave structure of Van Leer's solution, Roe's method can produce the carbuncle or not. More precisely, a subcritical shock profile, in which the intermediate shock point is closer to the downstream state does not produce the carbuncle (Fig. 3(c)). Also, a supercritical shock profile, in which the intermediate shock point is closer to the upstream state does result in a carbuncle solution (Fig. 3(d)). A Van Leer subcritical shock profile is observed when internal points are close to the downstream state (Fig. 4). Finally, it should be acknowledge that between the two results obtained with Roe's method (Figs. 3(c) 3(d)) a full range of solution is available, in which the carbuncle phenomenon is more or less visible. The present method based on Van Leer's subcritical shock profile cannot be regarded as a practical cure since it would require several *ad hoc* gridlines adaptation of the bow shock.

4. CONCLUSION

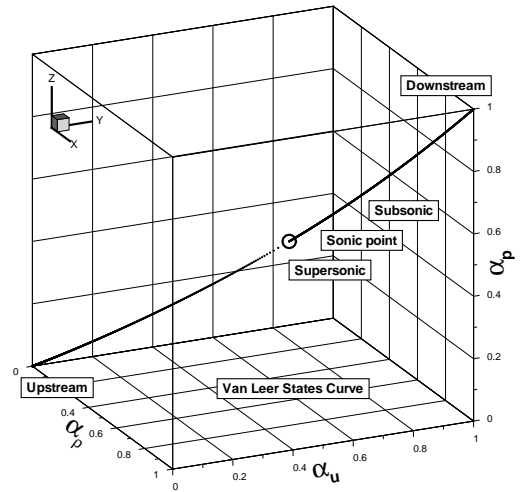
The present analysis provides a clue to explain why, in the blunt body problem, certain grids lead to carbuncle solutions while others do not. Also, the effect of the internal shock structure on shock instabilities indicates that one might cure the carbuncle phenomenon by simply acting on the 1D form if the numerical flux function without degrading the contact-preserving property.

REFERENCES

1. Quirk, J. J. A Contribution to the Great Riemann Solver Debate. *International Journal for Numerical Methods in Fluids* 1994; 18:555-574.
2. Gressier J, Moschetta JM. Robustness versus accuracy in shock wave computations. *International Journal for Numerical Methods in Fluids* 2000; 33:313-332.
3. Kim SS, Kim C, Rho OH, Hong SK. Cures for the shock instability: Development of a shock-stable Roe scheme. *Journal of Computational Physics* 2003; 185:342-374
4. Dumbser M, Moschetta JM, Gressier J. A matrix stability analysis of the carbuncle phenomenon. *Journal of Computational Physics* 2004; 197(2):647-670
5. Xu K, Li Z. Dissipative mechanism in Godunov-type schemes. *International Journal for Numerical Methods in Fluids* 2001; 37:1-22.
6. Karni S, Čanić S. Computations of slowly moving shocks. *Journal of Computational Physics* 1997; 136:132-139.
7. Arora M, Roe PL. On postshock oscillations due to shock capturing schemes in unsteady flows. *Journal of Computational Physics* 1997; 130:25-40.
8. Roe PL. Fluctuations and signals - A framework for numerical evolution problems. In *Numerical Methods for Fluid Dynamics*, Morton KW, Baines MJ (eds). 1982; 219-257
9. Wada Y, Liou MS. An accurate and robust flux splitting scheme for shock and contact discontinuities. *SIAM Journal on Scientific Computing* 1997; 18(3):633-657

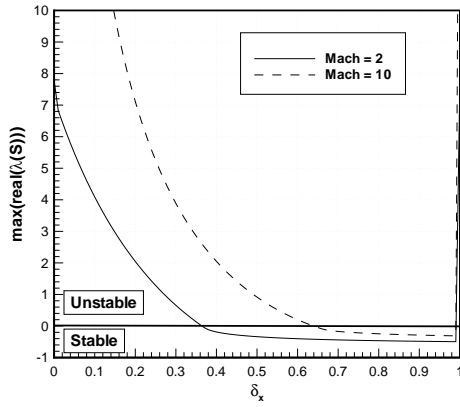


(a) Godunov, Roe, HLLC

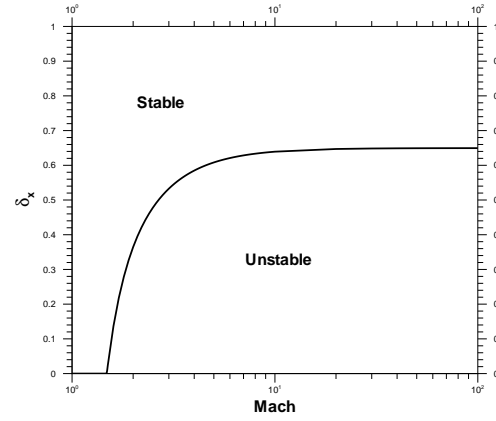


(b) Van Leer

Figure 1. 1D shock numerical structures - $M_0 = 2$ - primitive states ratios



(a) Stability as a function of the internal point location



(b) Stability diagram: effect of Mach number and internal point location

Figure 2. effect of shock numerical structure on 2D stability - Godunov, Roe, HLLC - 25×25 grid

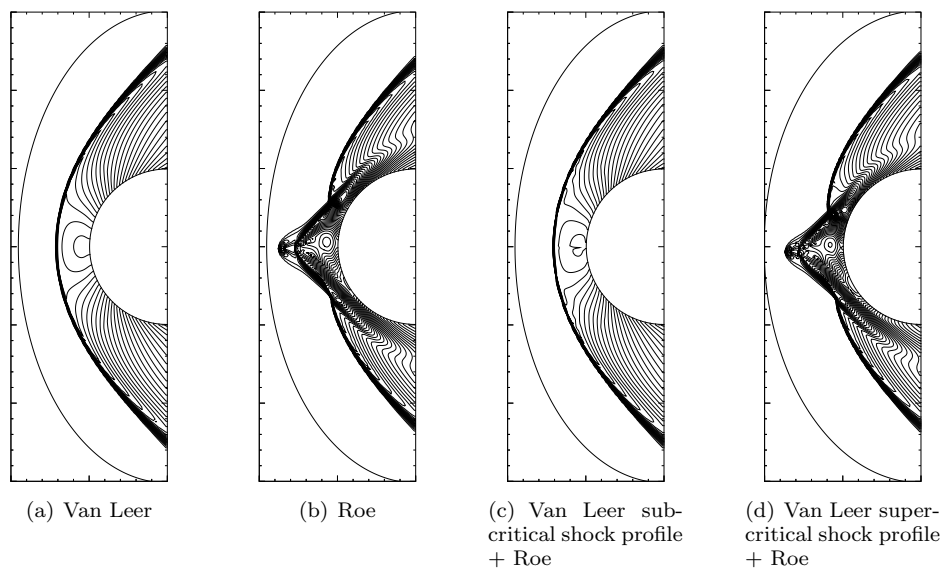


Figure 3. effect of shock numerical structure on the carbuncle phenomenon - $M_\infty = 10$ - density

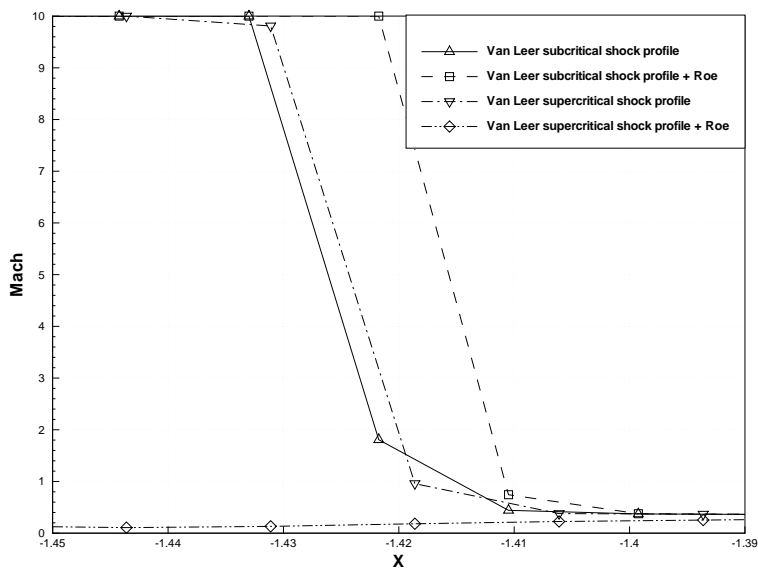


Figure 4. Shock numerical structure along symmetry line ($Y = 0$)- $M_\infty = 10$